JOURNAL OF APPLIED ELECTROCHEMISTRY 21 (1991) 189–202

REVIEWS OF APPLIED ELECTROCHEMISTRY 25

The refining of lead by the Betts process

J. A. GONZÁLEZ-DOMÍNGUEZ, E. PETERS*, D. B. DREISINGER

Department of Metals and Materials Engineering, The University of British Columbia, 309–6350 Stores Road, V6T 1W5 Vancouver BC Canada

Received 17 October 1989; revised 10 May 1990

Current extractive metallurgy techniques for lead refining by the Betts Electrorefining Process (BEP) are reviewed. In the BEP, refined lead (> 99.99%) can be produced by the electrorefining of impure lead anodes. The process relies on the selective dissolution of lead which leaves behind a strong and adherent layer of solids (slimes) containing the noble impurities originally present in the anode. The properties of this layer are closely linked to the physical metallurgy of the lead anode. Careful control of microstructure and level of impurities in the lead anode is required, and an essential attribute of the process is the use of the H_2SiF_6–$PbSiF_6$ electrolyte. This paper focuses mainly on the relationship between the anodic process and its effects. The effect of impurities and electrolysis parameters on the cathodic process are also reviewed. Descriptions of industrial operations of the BEP throughout the world are tabulated.

1. Introduction

This paper deals mainly with the Betts electrorefining process for lead, as described in the literature. In this process lead bullion is purified by transferring most of the lead from a soluble anode to a cathode through a lead containing electrolyte while leaving behind impurities in an adherent anode slime. The electrochemistry of this process involves the properties of anode slimes and of entrained electrolyte. Thus, the processes of anodic corrosion of lead and transport of lead ions through the entrained electrolyte are essential to the understanding of the Betts process. In this review, the physical metallurgy of lead anodes, which affects the slimes adherence is also discussed.

2. The extractive metallurgy of lead

Lead is an ancient metal. It was used by the Romans for components of their water distribution systems because of its malleable and ductile properties [1]. The ancients made lead of acceptable purity probably by smelting lead ores under conditions that prevented arsenic, antimony, and other hardening elements from reducing to the metallic phase. This could be accomplished in most cases by producing high lead slags such as those still produced in fire assaying. In those days it was necessary to avoid excessive copper in the ore, but arsenic, antimony, bismuth, nickel, iron, etc. were reliably held in the slag by maintaining the high oxidizing conditions of lead silicate based slags. Lead recoveries were low – not better than 85% from the highest grade hand picked galena ore. When high lead recoveries were found to be obtainable by coke-based blast furnace reduction, lead so produced was too hard, usually because of its copper, antimony, and arsenic content. The function of lead refining became both a softening process and a method of recovering silver and gold [2].

Nowadays the extraction process can be conveniently portrayed in the two step flowsheet shown in Fig. 1. The first step involves bullion production from the sulphide concentrate and the second step the refining of bullion to the final product.

The conventional route for bullion production requires sintering of the concentrate to produce a lead oxide containing product, which is then reduced in a blast furnace with metallurgical coke to produce lead bullion. The KIVCET and QSL processes represent two relatively recent commercial developments [3] that replace both the sintering–blast furnace combination with a single furnace that treats concentrates, and reduce both the costs of lead smelting and the environmental impact.

The KIVCET [4] process replaces the sintering/blast furnace operations with a flash smelting step. In this process, lead sulphide is oxidized to lead bullion and sulphur dioxide in a stream of oxygen. In a second step, the bullion and slag flow under a weir to an electrically heated settling hearth where coke breeze or coal is added to reduce the residual lead oxide in the slag and produce a final bullion (for refining) as well as a low-lead slag.

The QSL [5] process consists of a long, horizontal, tubular, brick-lined converter in which lead concentrates are pelletized and injected near one end into a bath containing lead bullion, lead oxide-containing slag, and lead sulphide matte. Oxygen is blown into the bath in the feed injection (and lead-bullion discharge) zone where it ultimately oxidizes sulphide sulphur to sulphur dioxide gas. Slag is tapped from the far end of the reactor after passing through a zone

* To whom all correspondence should be addressed.

0021-891X/91 $03.00 + .12

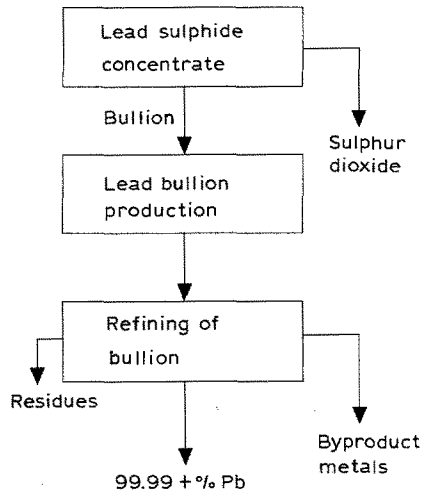

Fig. 1. Flowsheet for lead extraction from sulphidic concentrates.

where reducing coal-air mixtures are injected through tuyeres to lower its lead oxide content.

The refining of bullion is carried out by either a pyrometallurgical route or a combined pyrometallurgical/electrometallurgical route. Comparisons between these two routes show that the pyrometallurgical route is usually used when ores with low bismuth content are treated [7, 8]. The generalized pyrometallurgical flowsheet is shown in Fig. 2. This process consists of a series of steps which capitalize on a complex series of phase relationships to extract all the impurities contained in the lead bullion down to very low levels. Reviews on the chemistry and technology of these refining steps are available in the literature [4, 6, 9–11].

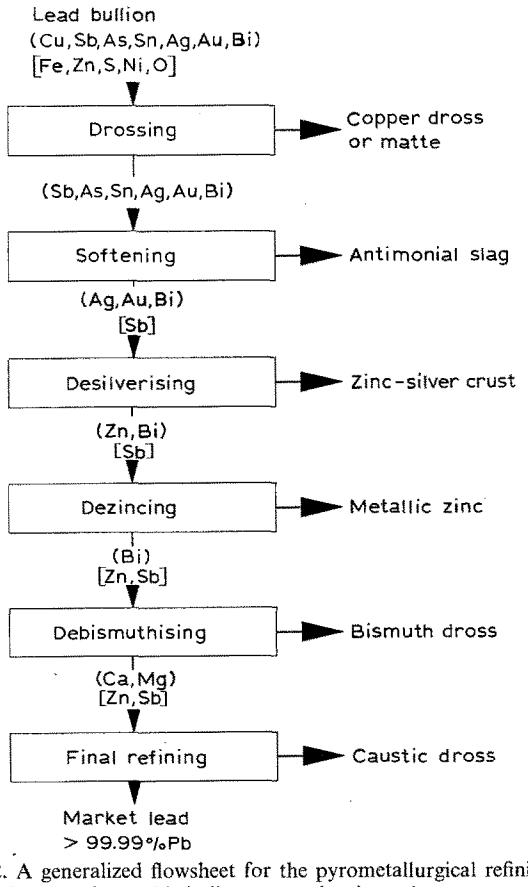

Fig. 2. A generalized flowsheet for the pyrometallurgical refining of lead. Parentheses ( ) indicate a major impurity component. Brackets [ ] indicate a minor impurity component [6].

The combined pyrometallurgical/electrometallurgical route is shown in Fig. 3. Here, copper drossing is performed to remove the bulk of the copper as a combination of matte and arsenide-antimonide for further treatment, thus allowing for the removal of some arsenic and antimony. Arsenic and antimony are sometimes reduced further as sodium arsenate-antimonate dross by oxidizing in the presence of caustic soda, because their levels in bullion must be controlled to produce suitable anodes for successful electrorefining practice.

Electrorefining is carried out in either a fluosilicic, fluoboric or sulphamic acid electrolyte and produces a commercial lead cathode product and an anode with an adhering slime [12]*. The purity of the produced lead is usually higher than 99.99% [13]. The slimes, representing only 2 to 4% of the anode weight, are treated by a variety of processes to recover silver, copper, antimony, gold, bismuth, and sometimes tin and indium [14–21].

Processes that entirely avoid smelting (and its attendant gas and dust treatment systems and associated environmental risks), utilizing hydrometallurgical/electrometallurgical flowsheets, have also been proposed to replace the current technology [23]. These include (a) the US Bureau of Mines ferric chloride leach process [24] which recovers lead via the molten salt electrolysis of $PbCl_2$, (b) the Minemet Recherche ferric chloride leach process [25] which recovers lead from chloride leach solutions using aqueous electrolysis and (c) the US Bureau of Mines process [26] for leaching lead concentrates in waste fluosilicic acid with an oxidant (hydrogen peroxide or lead peroxide) followed by aqueous electrolysis from the fluosilicic acid leach solution. All these processes have been piloted, but none has been commercialized†.

3. Plant practice in lead electrorefining

A detailed description of the Betts Electrorefining Process (BEP) can be found in Betts' book [27] and numerous patents [28–32]. The fundamentals of the process described there remain applicable to all the plants which currently electrorefine lead.

The BEP process is used in Canada [33–36], China [22, 37, 38], East Germany [39], Italy [40–42], Japan [43–51], Peru [52–54], Rumania [55, 56], Russia [57–59], USA [60] and West Germany [61–63]. The average annual production of lead by BEP is approximately 1 000 000 tons. Since the production of refined lead in the non-socialist countries (for which good figures are available) is close to 4 700 000 tons per year [64], it can be assumed that up to about 20% of world lead production is refined by the BEP. Two variations of the

* Nitric acid media is not suitable because, in the presence of free acid, nitrate is reduced (to nitric oxide gas) at the cathode, preferentially to plating of lead. At higher pH, where the nitrate ion is much more inert to reduction, the electrical conductivity of the electrolyte is much too low for an economic practice.

† Commercialization of any new lead processes faces a lack of need for plant expansion in this industry and so must be justified on the basis of conversion or replacement of existing capacity.

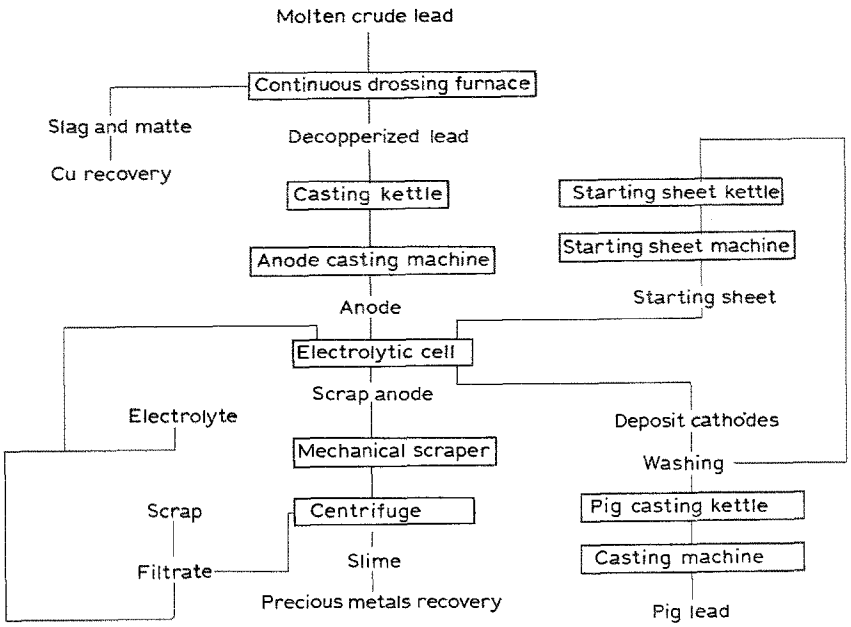

Fig. 3. A generalized flowsheet for the pyrometallurgical/electrometallurgical refining of lead [22].

BEP, the sulphamic acid and the fluoboric acid processes are operated in Italy [41] and in West Germany [61] respectively.

The Betts Electrorefining Process normally utilizes a fluosilicic acid (H_2SiF_6) electrolyte containing lead fluosilicate to electrorefine impure lead anodes into pure lead cathodes. The fluoborate and the sulphamate processes are identical to the fluosilicate process except for the substitution of the electrolyte. Fluoboric acid has not been extensively used due to its relatively high cost. HBF_4 is a stable acid with a good electrolytic conductivity and a high solubility of the lead salt. It is also used in lead plating baths [65–67], lead fluoborate-fluoboric acid rechargeable batteries and in the recovery of lead from spent batteries [68–72].

The sulphamic acid process has two main limitations when compared to the fluosilicic acid process [40, 58, 73]: firstly, sulphamic acid decomposes rapidly at current densities larger than $100\,A\,m^{-2}$ resulting in high reagent replacement cost; secondly, the free acid is a crystalline solid of limited solubility, and limited ionization in aqueous solution, leading to a low conductivity of sulphamic acid solutions (at most, half of the conductivity of equivalent fluosilicic acid solutions). This results in larger power costs in refining. The significant advantage of the sulphamic acid process is that it is the most efficient process for the removal of tin from impure lead (Sn remains in the slimes) [74–77]. Plants that use the fluosilicic process remove Sn prior to electrolysis by using the Harris process [78]. When anodes containing significant Sn concentrations are refined by the Betts process, tin dissolves with lead at the anode and co-deposits at the cathode. The lead-tin alloy may be sold, or some post treatment of the cathodes is necessary to remove the tin [79].

The wide use of H_2SiF_6 in lead electrorefining is due to its low cost. Fluosilicic acid is produced as a by-product of the treatment of phosphate rock in fertilizer manufacture [80]. Fluorides and silica containing in phosphate rock form fluosilicate and are separated from the fertilizer product. Fluosilicic acid is also produced as a by-product during the dissolution of apatite with sulphuric acid [54, 80]. During the electrorefining operation, fluosilicic acid is consumed by entrapment in the anode slimes and by volatilization from the surface of the electrolyte. The acid develops significant vapour pressures through volatile decomposition products according to the reaction,

$$H_2SiF_6 \longrightarrow 2HF(g) + SiF_4(g)$$

SiF_4 and HF are both corrosive and toxic and are removed from the tankhouse atmosphere by adequate ventilation.

Table 1 shows some of the operating parameters of various lead electrorefining plants. The wide variation in electrolysis conditions seen in this table does not seem to have a strong influence on the final quality of the refined lead. For example, lead concentrations in the electrolyte can be varied between 30 and $270\,g\,l^{-1}$ without affecting seriously the refined lead quality. The electrolyte recirculation rates are also varied widely, with no apparent correlation to other operating parameters. Extremely high electrolyte velocities might improve mass transfer across electrode boundary layers, but can also nullify the additive effects, worsening the deposit quality and causing short circuits [81].

Table 1 also shows that the current densities employed in the Betts process fall in the range of 120 to $230\,A\,m^{-2}$. Higher current densities have been achieved through the use of galvanodynamic techniques such as current modulation and periodic current reversal (PCR). The current modulation technique consists of decreasing the current density (for example, from 220 to $160\,A\,m^{-2}$) in small steps [33, 87]. Each constant current density step is determined on the

Table 1. Betts lead electrorefining in the world

	Takehara, Japan [43]	*Chigirishima Japan [47]*	*Harima Japan [46]*	*Shenyang Smelter, China [82]*
Electrolyte				
Pb ($g l^{-1}$)	236–270	75	90–100	74
Total H_2SiF_6 ($g l^{-1}$)		135		104–124
Free H_2SiF_6 ($g l^{-1}$)	52–61		110–115	38–58
Others: ($mg l^{-1}$)	2–5 Bi, 0.5–2Cu, 1–2 As, 130–200 Sb			400 Sb, 800 Fe, 110 As, 28 Zn, 290 Sn, 0.2 Ag
Additives Consumption:				
Aloes ($g ton^{-1}$)				
Lignin sulphonate ($g ton^{-1}$)			1000	300–450
Glue ($g ton^{-1}$)	600–1100			200–300
Others ($g ton^{-1}$)				β-naphtol
Temperature (°C)	28–43	35–38	40–43	32–45
Circulation apparatus			$1.8 m^3 min^{-1} \times 20 m$ Head	Pressure tank with centrifugal copper pump
Recirculation rate ($l min^{-1}$)	30	40	30	18–25
Acid loss ($kg ton^{-1}$)	1.6–2.7	2.3	4	1.5–1.7
Current				
Cathode ($A m^{-2}$)	120–140	147	185	154–172
Cell voltage (V)	0.5–0.6	0.47	0.55	0.46
Current (KW per Generator)	15000 A at 70 V	10000 A at 200 V	5000 A at 50 V 13000 A at 50 V	2800–3500
Current efficiency (%)	95.6–98.7	93	93	96.30
Energy consumption ($kWh ton^{-1}$) Pb:			175–180	
Electrolysis	154–157	143		120–130
Mechanical	17.8–20.7	30		30–40
Anodes				
Casting technique	Casting wheel, 18 moulds	Vertical casting with water cooling on top of the mould	Casting wheel with water cooling on top and bottom of the mould, 15 mould	Casting wheel
Composition	0.98% Sb, 0.5% Bi, 0.02% Cu, 0.02% Sn, 0.01% As, 67 oz ton^{-1} Ag, 0.4 oz ton^{-1} Au	1.25% Sb, 0.12% Bi, 0.06% Cu, 65 oz ton^{-1} Ag, 0.07 oz ton^{-1} Au	0.5% Sb, 0.13% Bi, 0.1% Cu, 0.05% Sn, 0.05% As	0.68% Sb, 0.073% Cu, 0.044% Sn
Length, width, thickness (mm^3)	1150 × 1000 × 25–39	1200 × 800 × 24	970 × 740 × 35	920 × 620 × 23
Mode of suspension	Cast lugs	Cast lugs	Cast lugs	Suspended lugs
Life, days	8 (half cycle scrubbing)	7	8	5
Scrap (%)		30	26.5	20–25
Anode spacing (mm)		100	110	95
Weight (kg)	380–440	250	280	140 ± 3
Cathodes				
Thickness (mm)	0.6–1.0	0.8	1	0.8–1
Weight (kg)	10–20	10	10	8–11
Life (days)	4–5	7	4	2.5
Anode slimes				
Composition	36.9% Sb, 17.4% Bi, 12.1% Pb, 3.1% Cu, 0.1% Sn, 0.4% As, 8.9% Ag, 0.06% Au	45% Sb, 4% Bi, 12% Pb, 3% Cu, 7–10% Ag, 3.22 oz ton^{-1} Au, 30% H_2O		12–15% Pb, 8–12% Bi, 0.2–0.4% Te
Removed after ? days	4	7		2.5
Percentage of anodes	2.4–3.6	2.9	1.3	1.1–1.4
Scrubbing technique	Rotating brush			
Tanks				
Length, width, depth (cm^3)	500 × 130 × 155	300 × 100 × 150	1150 × 920 × 1450 (inner size)	320 × 75 × 120
Number of anodes, cathodes	42, 43	28, 29		32, 33

Table 1. Continued

	Takehara, Japan [43]	*Chigirishima Japan [47]*	*Harima Japan [46]*	*Shenyang Smelter, China [82]*
Construction materials	prefabricated concrete, PVC lining	vinyl chloride with steel frame	asphalt lined reinforced concrete tank	Reinforced concrete with asphalt or PVC lining
Pb Annual production(ton)	45000	68000	27000	54450
Pb Average content (%)	99.999	99.999	99.999	99.99+
	Cominco, Canada [83]	*'Albert Funk', East Germany [84]*	*Cerro del Pasco, Peru [85]*	*Kamioka, Japan [86]*
Electrolyte				
Pb ($g l^{-1}$)	75 (60–80)	30–50	75	75
Total H_2SiF_6 ($g l^{-1}$)	141	120	120	130
Free H_2SiF_6 ($g l^{-1}$)	90 (90–100)	100	60	75
Others: ($mg l^{-1}$)	8 Bi, 65 Sb, 4000 SiO_2, 1.6 Cu, 12 Sn, 5 As, 17 In, 70 Tl		600 HF, 5 Sb, 5 Bi, 0.5 SiO_2, solids	1 Bi, 150 Sb
Additives Consumption:				
Aloes ($g ton^{-1}$)	170 (Aloin)			
Lignin sulphonate ($g ton^{-1}$)	250 (Calcium)		500 (Calcium)	180
Glue ($g ton^{-1}$)		600	550	600
Others ($g ton^{-1}$)				
Temperature (° C)	40 (38–43)	35	40	35–45
Circulation apparatus	Centrifugal pumps	Storage tank with epoxy lined pump	Centrifugal pumps	Volte pump 18.5 kW × 2
Recirculation rate ($l min^{-1}$)	27 (27–45)	10	12	40
Acid loss ($kg ton^{-1}$)	2	15 (32% pure)	3	2
Current				
Cathode ($A m^{-2}$)	230 (max)	185	156	135
Cell voltage (V)	0.3–0.5	0.45	0.5–0.6	0.55
Current (KW per Generator)	6300 A (5 day), 5400 A (7 day) 1000 kW	150	Mercury rectifier 1520 motor generator 360	20000 A at 60 V
Current efficiency (%)	90–95	92	90	96
Energy consumption ($kWh ton^{-1}$) Pb:				
Electrolysis	168	195	143	165
Mechanical	50	90	35	130
Anodes				
Casting technique	Open mould casting wheel	Casting wheel, 12 mould	Casting wheel	Horizontal casting with horizontal mould
Composition	1.2–1.4% Sb, 0.4% As, 0.15% Bi, 0.05% Cu, 100 oz ton^{-1} Ag	0.5% Sb, 0.3% Ag, 0.3% Bi, 0.1% Cu, 0.002% Sn	1.8% Sb, 0.15% As, 1.5% Bi, 0.05% Cu, 0.01% Sn, 0.07 oz ton^{-1} Au, 140 oz ton^{-1} Ag	0.4% Ag, 0.3% Bi, 0.1% Cu, 0.6% As, 0.6% Sb
Length, width, thickness (mm^3)	864 × 660 × 30	730 × 710 × 25 (immersed surface)	940 × 690 × 25	1140 × 990 × 20
Mode of suspension	Lugs designed into casting	Suspended lugs	Suspended lugs	Shoulder type
Life, days	5	6	4	6
Scrap (%)	25	40	49	45
Anode spacing (mm)	100	130	100	110
Weight (kg)	206	200	150	
Cathodes				
Starting sheet Production technique	Continuous drum casting	Mechanized production with on line casting or ribbon	Continuous drum casting	Direct method machine
Thickness (mm)	1	1	0.6	0.7
Weight (kg)	6.3	60–70 (Final weight)	80 Final weight	13
Life (days)	5 or 7	3	4	6

Table 1. Continued

	Cominco, Canada [83]	*'Albert Funk', East Germany [84]*	*Cerro del Pasco, Peru [85]*	*Kamioka, Japan [86]*
Anode slimes				
Composition	40% Sb, 16% As, 13% Pb, 2.5% Cu, 2500 oz ton^{-1} Ag	15% Pb, 25% Sb, 15% Ag, 10% Bi, 5% Cu	28% Sb, 10% As, 24% Bi, 10% Ag, 1.2% Cu, 0.07% Se, 0.52% Te, 18% Pb, 38.4% H_2O, 0.4% SiO_2	10% Pb, 15% Ag, 15% Bi, 1% Cu, 20% As, 20% Sb
Removed after ? days	5 or 7	6	4	6
Percentage of anodes	3	1% (solids)	4	1.4
Scrubbing technique	conveyed by monorail between rubber scrapers	pneumatic stripping	Water sprays	Rotating brush
Tanks				
Length, width, depth (cm^3)	268 × 82 × 112	230 × 80 × 120 (inner size)	455 × 95 × 130	500 × 130 × 160
Number of anodes, cathodes	24, 25	16, 17	40, 41	43, 44
Construction materials	Asphalt lined concrete (old) polymer concrete (new)	Rubberized steel plates	Glue lined concrete	Vinyl chloride resin and concrete
Pb Annual production(ton)	144000	15000	72000	30000
Pb Average content (%)	99.99	99.99	99.99	99.99

basis of an anode overpotential value which increases as the slimes layer thickens and decreases when the current density is reduced. The upper limit for the anode overpotential is usually determined by bismuth dissolution from the anode. Figure 4 shows the current density program that can be applied to the electrorefining circuit without reaching the critical overpotential value for bismuth dissolution. The higher average current density possible with current modulation reflects in a shorter electrorefining cycle and higher refinery production.

Periodic current reversal (PCR) in lead electrorefining is widely employed in China [38]. PCR involves frequent short reversals of the electrolysis current direction [88]. This reduces the concentration polarization in the slimes layer and levels the cathodic deposit by selectivity dissolving projections. High current efficiencies, good cathode quality, low electrolyte losses, low energy consumption and a decrease in the number of short circuits has been reported through the use of PCR [22]. A 16% increase in free acid was found in the slimes layer due to PCR [22].

4. The anodic process

4.1. *Introduction*

The Betts process, as practiced by all refineries, depends on the formation of an adherent, porous anode slimes layer during electrolysis. The slimes layer consists of undissolved impurities which are removed mechanically from anode scrap after the anodes are withdrawn.* If the slimes do not adhere to the anode

* During normal lead electrorefining practice some slimes do fall, and are cleaned out of the cells at very infrequent intervals (months).

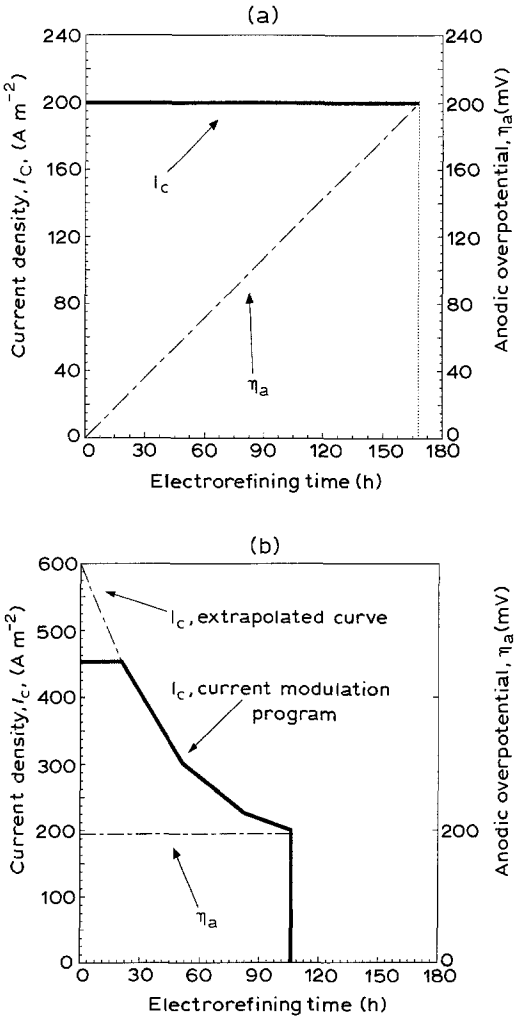

Fig. 4. Changes in the anodic overpotential value, η_a, during lead electrorefining: (a) conventional galvanostatic process (b) galvanodynamic process in which the cell current is continuously decreased during the refining cycle to fix the value of η_a [87].

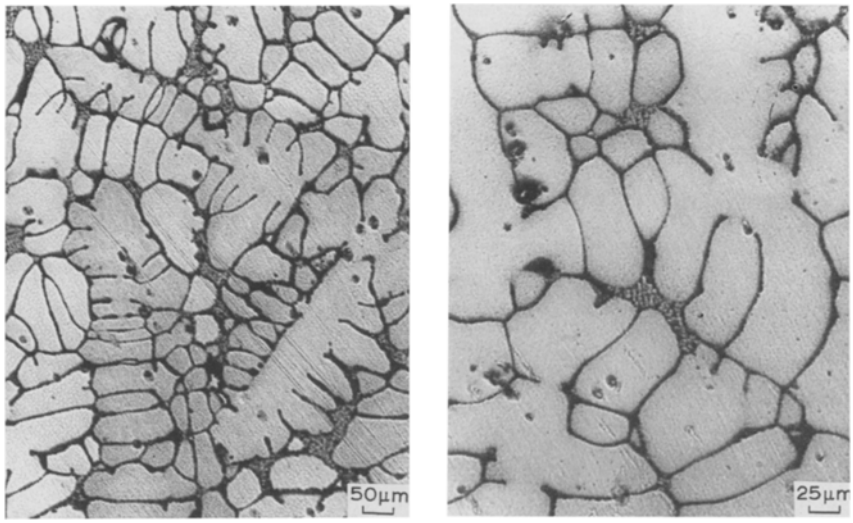

Fig. 5. Lead anode microstructure. From an anode currently being used by Cominco Ltd. Chemical composition as described in Table 1. Top view, air cooled side.

during electrolysis they will settle through the solution and to some extent be mechanically entrained in the cathode deposit. There is no indication in the literature of a lead refining process in which (as in copper refining) slimes fall is encouraged. Further, the recovery of slimes from the bottom of the cell (as in copper refining) is perceived to be more costly. To form an adherent slimes layer, certain elements (mainly As, Sb, and Bi) must be controlled within a narrow composition range and/or ratio in the anode, and the anode casting process must be designed to control the rate of solidification to optimize the microstructure of the cast bullion.

4.2. *The physical metallurgy of the lead anodes*

The lead anode microstructure that is desired for optimum slimes structure during electrorefining is known as the honeycomb structure, because it consists of uniform size grains of lead surrounded by impurities on the grain boundaries (Fig. 5). As the lead grains dissolve they leave behind a skeleton of slimes which resembles a honeycomb. Any non-uniformity of the matrix will lead to non-adherence of the slimes layer, and any precipitates present in this matrix material will contribute to slimes detachment because of their extra weight.

There are four elements present in the lead anodes that seem to exert a strong influence on the anodic process: As, Sb, Bi and Ag. The interaction of these impurities with each other and with lead can be deduced from the available binary and ternary phase diagrams [89–93], which show that both intermetallic compounds and eutectic structures may be present. Three different slime forming systems have been identified and classified from studies on synthetic anodes [94]:

(i) impurity phases of the solid solution type (SST): the Pb–Bi system.

(ii) impurity phases of the precipitation type (PT): the Pb–Sb system.

(iii) impurity phases of the eutectic type (ET): the Pb–As and the Pb–Ag systems.

The strength of slimes adhesion to the anode was quantified by Tanaka [94] through observations of slimes fall and slimes morphology. Tanaka summarized the results of these studies with the following relationships:

(1) The greatest slimes adherence is obtained when impurity phases of the SST type are present in the anode in concentrations greater than 0.23% by wt. A SST concentration lower than this critical value produced a slime that easily slides off the anode.

(2) The addition of a third element to the eutectic systems increases significantly the slimes adherence.

(3) Water quenching of the anodes increase slimes adhesion particularly in the PT and ET system cases. However, the very small slimes particles formed during quenching may also promote slimes detachment and mechanical entrainment in the cathodes.

The increase of slimes adhesion by water quenching relates directly to the lead anode solidification rate, which influences the growth and distribution of impurity-containing phases. Especially important are the eutectic forming systems where it is known that the solidification parameters (growth velocity, temperature gradient in the liquid and growth mechanism) and system parameters (volume fraction and impurities content) can lead to anomalous eutectic structures [95]. Such structures have been reported to occur in the following systems [95]:

Ag–Pb and Ag–Bi: broken lamellar structure type
Pb–Bi: complex structure type
Pb–Sb: complex regular structure and irregular structure type.

It must be emphasized that even though the physical metallurgy of the lead anodes is of great importance to the Betts process, there remains a lack of knowledge in this area.

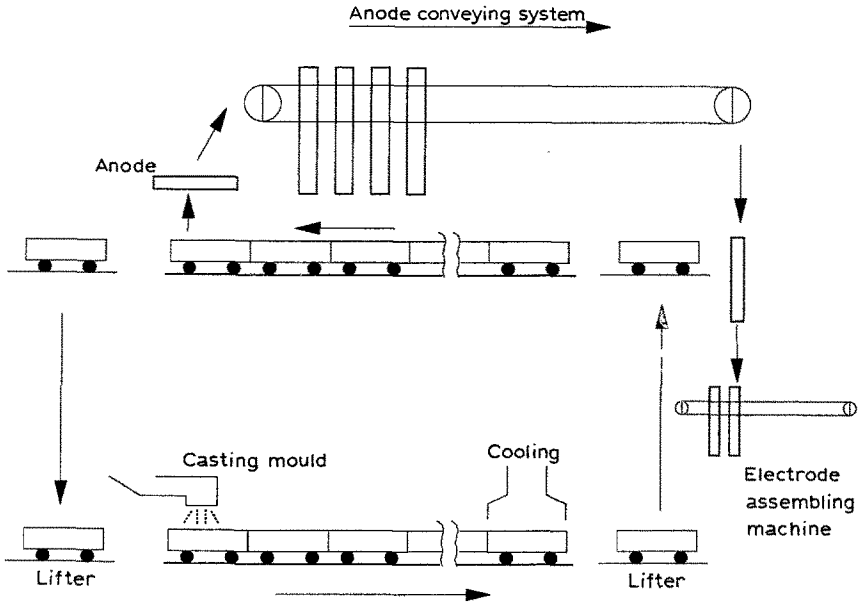

Fig. 6. Straight type horizontal lead anode casting system [44].

4.3. *Industrial practice*

As Table 1 shows, the range of anode impurities used in lead refining varies from plant to plant. In every refinery the anode composition is kept within narrow limits to obtain an adherent slimes layer. The need for production of anodes with homogeneous properties has led to control methods for cooling rates and casting techniques. In addition to the use of a casting wheel, straight horizontal [44–46] and vertical [47] anode casting systems are employed.

Figure 6 shows the straight type horizontal lead anode casting system currently used in Japan. Although the vertical and horizontal casting processes were originally developed to save space (over that occupied by a casting wheel), they were carefully designed to achieve uniform cooling rates during the casting of the anodes. Such new techniques for anode casting as well as for optimizing heat treatment have been patented by Japanese companies [96], but no information was found that would indicate the nature of changes in microstructure resulting from these newer techniques.

4.4. *Slimes electrochemical behaviour*

The slimes layer formed in the BEP undergoes structural and chemical changes during its growth. As the slimes layer thickens, the different phases and compounds present react with the entrained electrolyte creating secondary products. The E_h-pH diagram for the $PbSiF_6$–H_2SiF_6 system [101] indicates that both lead fluoride and silica can precipitate at higher pH values. This has been related to the effect of electrolysis parameters on secondary processes (such as these precipitations) that take place within the slimes layer during electrolysis [97–100]. The transport processes within the slimes layer in the context of these secondary reactions has also been the subject of several studies [102–108].

A simple physical model to study the role of the slimes layer during anodic dissolution rate in electrorefining systems was developed by Reznichenko *et al.* [109]. In this model, the slimes layer was represented by a silver gauze diaphragm (representing the noble impurity) electrically connected to the anode (a highly pure base metal) and placed at a (variable) distance from the anode corresponding to the slimes – electrolyte interface. The distance between the anode and the gauze was varied to simulate the effect of an increasing ohmic drop between the anode and the slimes layer. During electrolysis, concentration gradients normally present in a slimes layer were replaced by a simple concentration difference between the solutions on the two sides of the gauze, and this was related to a modified Nernst equation:

$$\ln [Me_2^{n_2^+}] = \left(E_1^0 - E_2^0 + \Delta\phi + \frac{RT}{n_1 F} \ln [Me_1^{n_1^+}]\right) \frac{n_2 F}{RT} \quad (1)$$

where: $[Me_2]$, n_2 = concentration and valence of noble metal; $[Me_1]$, n_1 = concentration and valence of base metal; $\Delta\phi$ = ohmic drop between the base metal and the noble metal gauze; E_1^0 = rest potential of the metal to be refined; E_2^0 = rest potential of the noble metal; F = Faraday's constant; R = gas constant; and T = temperature.

Equation 1 shows that the larger the ohmic drop the larger the equilibrium concentration of ions of the noble metal and the larger its dissolution rate. Although this model oversimplifies the different phenomena taking place within a slimes layer, it provides an insight as to the effect of ohmic drop buildup in the slimes layer and the dissolution rate of noble impurities normally left in the slimes. Reznichenko *et al.* [109] applied their model to the study of the Cu–Ag system in which they found a logarithmic relationship between the dissolution rate of noble impurities and the ohmic drop potential.

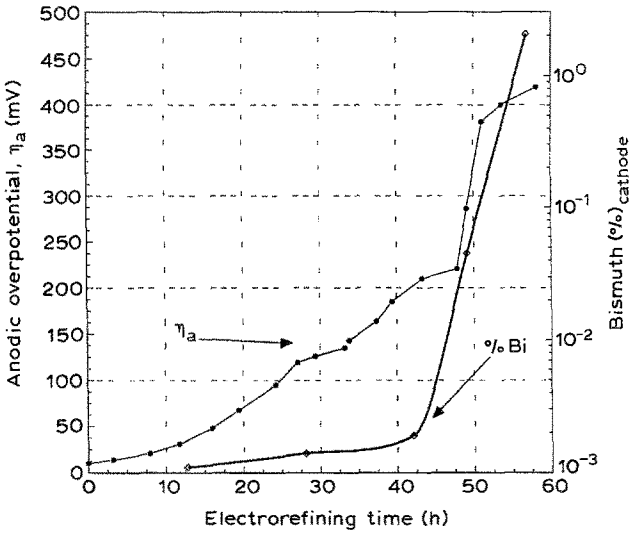

Fig. 7. Bismuth content of the cathodic deposit as a function of the anodic polarization and the electrolysis time. I_c = 170–350 A m^{-2}. Anode composition 8.4–11.2% Bi, remainder Pb [110].

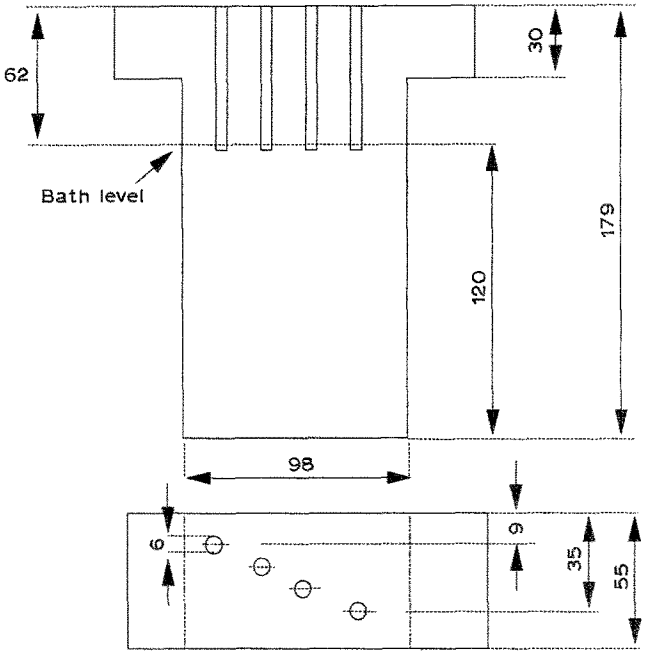

Fig. 8. Dimensions of the anodes used in Wenzel's experiments showing the position and size of the electrolyte sampling wells [97]. All measurements in mm.

Early research on the behaviour of BEP slimes has focused on relating the anodic overpotential to the cathode purity [110, 111]. Among the impurities most closely followed in the cathodic deposit is bismuth [112, 113]. Even though the BEP has a large selectivity for the removal of bismuth, it has been found that towards the end of the electrorefining cycle such selectivity can be lost. It seems that the buildup of concentration gradients and the precipitation of secondary products within the slimes layer can initiate steep increases or discontinuities in the anodic overpotential at a certain slimes thickness. This would produce a large increase in the rate of dissolution of such impurities, and subsequently in the deposition of impurities in the cathodic deposit. Figure 7 shows how bismuth contamination in the cathode increases with anodic overpotentials above a critical value (about 200 mV). This has been recognized as a general behaviour for bismuth in lead refining by the BEP [33, 87, 110, 111]. On the other hand, the use of periodic current reversal (PCR) [39, 98] has been found to increase the minimum anodic overpotential at which noble impurities start to dissolve.

Table 1 shows that the slimes layer weight is only 1 to 4% of the original anode weight; yet, they occupy the whole of the original anode volume. This indicates that the porosity of the slimes layer exceeds 92% and may be as high as 98% (taking into account a density for slimes phases of about half that of the bullion). Concentration gradients in the electrolyte confined within this highly porous layer and the slimes electrochemistry are closely linked.

Wenzel *et al.* [97, 114, 115] measured the change in composition of the electrolyte contained in the slimes layer as a function of time and of slimes thickness. Figure 8 shows the sampling method used by Wenzel, utilizing sampling wells at different distances from the anode surface. Small amounts of electrolyte were withdrawn through these wells at carefully selected times (to avoid perturbing appreciably the system).

According to their results, using a range of anode compositions (Bi from 0 to 1.74% and Sb from 0.45 to 3.01%), the more the amount of secondary solidified material (SSM) present in the anode, the steeper the pH and the Pb^{+2} concentration gradient throughout the slimes layer. Also they found that the thicker the slimes layer the steeper the concentration gradients. Figure 9 shows these changes in concentration for two different anode compositions. Wenzel *et al.* proposed that due to the pH increase several reactions may occur: SiF_6^{-2} decomposition to SiF_4 and F^- (pH > 3); precipitation of Sb_2O_3 (pH > 4.9) and precipitation of Pb_2O (pH > 7).

Table 2 shows the results of chemical and diffraction analysis, which seems to indicate the presence of these secondary compounds within the slimes layer*. From an analysis of the concentration of noble impurities in the entrapped electrolyte, Wenzel *et al.* were able to conclude that when the SSM exceeded 5%, as determined from the Pb–Bi–Sb ternary diagram, permissible impurities in the anode were too high to obtain an acceptable impurity level in the refined lead.

Wenzel's X-ray diffraction analysis on the slimes products agree with the findings of Isawa *et al.* [116, 117], who studied the slimes composition of synthetic and industrial lead anodes and found the presence of the following compounds:

Metallic Bi: in the Pb–Bi, Pb–Bi–As, Pb–Bi–Sb, and Pb–Bi–As–Ag systems;
Metallic As: in the Pb–As, Pb–Bi–As, and Pb–Bi–As–Ag systems;
Metallic Ag: in the Pb–Ag and Pb–Bi–As–Ag systems.

* Note that since slimes oxidize rapidly in air, the analysis may indicate oxide phases where metallic phases were present in the *in situ* slimes.

Table 2. Chemical composition and X-ray diffraction analysis of the lead anode slimes [97]

Sample no.	Anode composition (% wt) (rest Pb)	Slimes chemical analysis (% wt)					X-ray diffraction analysis
		Pb	Sb	Bi	F	Si	
1	0.46% Sb, 0.24% Bi	56.98	7.62	3.95	11.97	6.66	PbO, Sb_2O_3, PbF_2, Bi_2O_3
2	0.46% Sb, 0.24% Bi	58.02	9.40	4.28	14.09	3.33	PbO, Sb_2O_3, PbF_2, Pb_4SiO_4, Bi_2O_3
3	0.92% Sb, 0.24% Bi	56.57	6.81	5.55	11.27	6.65	PbO, Sb_2O_3, PbF_2, Bi_2O_3
4	0.92% Sb, 0.24% Bi	53.77	9.37	9.20	12.22	4.19	PbO, Sb_2O_3, PbF_2, Bi_2O_3

Also the presence of the Bi–Sb solid solution, of the ε and ε' phases of the Ag–Sb system, and of water soluble As and Sb (identified as As_2O_3 and of Sb_2O_3) were found in some of the above mentioned systems and in the slimes obtained from industrial anodes [116, 117].

One compound that has been difficult to characterize is Ag_3Sb [94], whose presence has been detected in both synthetic and industrial lead anodes. The morphology of this compound has been found to be a function of the anode cooling rate and of the electrolysis conditions.

The electrolyte used in lead electrorefining contains impurities whose concentration ranges from a few ppm and several gl^{-1}, and have their origin in the anode from which they are dissolved (i.e. Cu^{+2}, Sn^{+2}) or from the acid manufacturing process (i.e. phosphorous species). Their steady state concentrations in the electrolyte depend on the electrolysis parameters and slimes thickness. They can affect both the anodic and cathodic processes through changes in fundamental electrochemical parameters such as the exchange current density (i_0), the transfer coefficient (α), and the electrical double layer capacity (e.d.l.). Measurement of these parameters usually involve transient electrochemical techniques, such as polarization scans, current interruptions, and AC impedance studies.

Miyashita *et al.* [118–123] have extensively studied the influence of minor impurities and addition agents in the electrolyte used in lead refining. These studies focused on the determination of fundamental electrochemical parameters (i_0, e.d.l., and α) as a function of Sn^{+2}, Fe^{+3}, Zn^{+2} and glue, using a single current step transient method [118]. He found that under an oxygen atmosphere the presence of the above ionic species increased the anodic overpotential value. Thus, they may inhibit the dissolution of some noble species including lead.

When noble impurities present in the lead anodes transfer to the electrolyte they can be redeposited by cementing on less noble elements. While such redeposition is obscured during anodic dissolution, it can be inferred from corrosion measurements in the absence of a current. For example, the weight loss rate for a lead sample in the presence of dissolved bismuth has been observed in the HBF_4–$Pb(BF_4)_2$ system [66]. Figure 10 shows how bismuth concentrations as low as 2 mM enhance the corrosion rate of lead.

During the dissolution of the lead anodes in the BEP, bismuth and other noble impurities accumulate

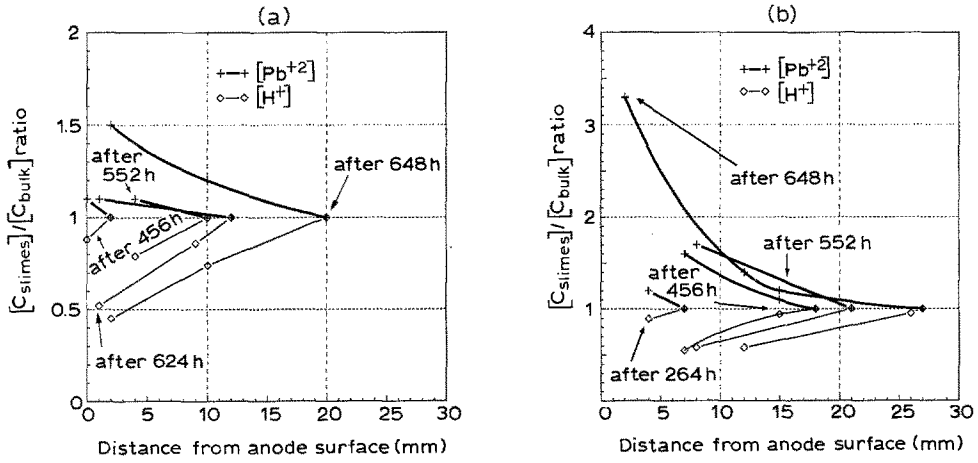

Fig. 9. Changes with electrolysis time of the relative concentrations of Pb^{+2} and H^+ within the slimes layer with respect to their bulk values. Bulk electrolyte composition: $[PbSiF_6]$ = 0.4 M, $[H_2SiF_6]$ = 1 M, T = 35° C, I = 200 a m^{-2}, stationary electrodes. Vertical axis: Pb^{+2} and H^+ concentration ratio between the electrolyte sampled within the slimes layer and the bulk electrolyte. (a) Anode with 0.46% Sb and 0.24% Bi ($\simeq$ 1.73% SSM), (b) anode with 0.92% Sb and 0.24% Bi ($\simeq$ 3.80% SSM) [97, 115]. Note: no extrapolation of the inner electrolyte concentrations at zero slimes thickness done here.

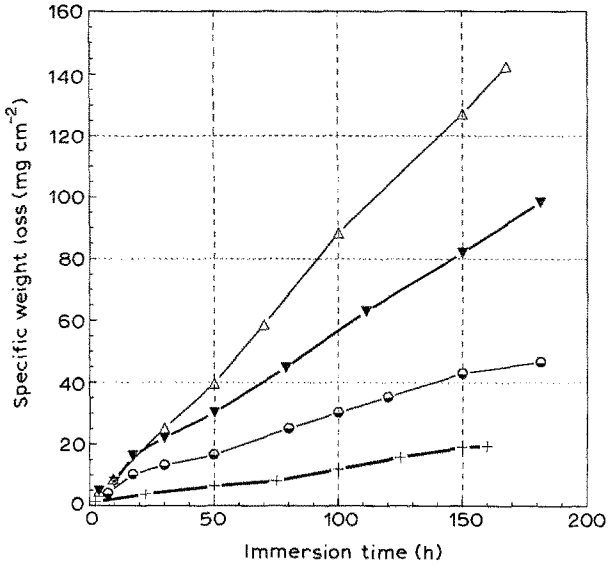

Fig. 10. Lead specific weight loss (corrosion) as a function of the immersion time in a 2 M Pb $(BF_4)_2$ – 1 M HBF_4 solution in the presence of (+) 0, (◒) 2, (▼) 5, and (△) 10 mM l^{-1} of Bi^{+3} [66].

in the proximity of the slimes-bulk electrolyte interface as well as in the bulk electrolyte [39, 124]. Since these noble impurities will deposit on the cathode at their limiting mass transfer rate, the permitted electrolyte concentration is related to cathode purity specifications (25 mg l^{-1} of bismuth will typically lead to 10 ppm bismuth in the cathode, [124]). They can be removed by one of two methods:

(a) Continuous cementation [125, 126] through a column filled with lead particles (Fig. 11).
(b) Electrodeposition in a separate electrolysis circuit [124]. The purified electrolyte is then sent to the main electrolyte stream. This method is being used in Japan [43].

The majority of plants that electrorefine lead do not purify their electrolyte, but rather, operate under conditions where the dissolution of noble impurities from the anode is limited to tolerable levels.

5. The cathodic process

5.1. *Additives control and electrochemistry*

In the absence of additives, lead deposits with a very small overpotential, and tends to form rough, porous deposits or dendrites that result in short circuits. To obtain deposits that are flat, smooth, and free from projections, special reagents are added to the electrolyte. These 'addition agents' increase the cathodic overpotential (actually called 'inhibition'), and change the kinetic parameters (i_0, α, and e.d.l.) under comparable electrolysis conditions [120–123].

Polarization measurements have been used for controlling and monitoring the concentration of additives in lead electrorefining circuits [81, 127–129], as well as for screening of additives in the electrolytic refining of copper and for testing of impurity levels in the electrowinning of zinc [130–134]. A polarization technique for determining lignin sulphonate in lead plating baths has also been described [135]. Long term studies and years of industrial practice, especially by Cominco researchers [81, 129] have lead to a sufficient understanding of the levelling mechanisms of lignin sulphonate and aloes, to permit the use of polarization measurements for controlling the concentration of these species in the industrial electrolyte for lead refining. This additives control is achieved by keeping the cathode polarization voltage (c.p.v.) within preset limits, and adjustments are made by either new additions or by regeneration (in the case of aloes) with a thiosulphate salt [128]. The level of additives present at a given time is directly related to the c.p.v.

5.2. *Starting sheet technology*

The cathode starting sheets used in the BEP are usually cast on a rotary drum casting machine. The stiffness of these sheets is increased by adding approximately 15 ppm antimony to the melt and by impress-

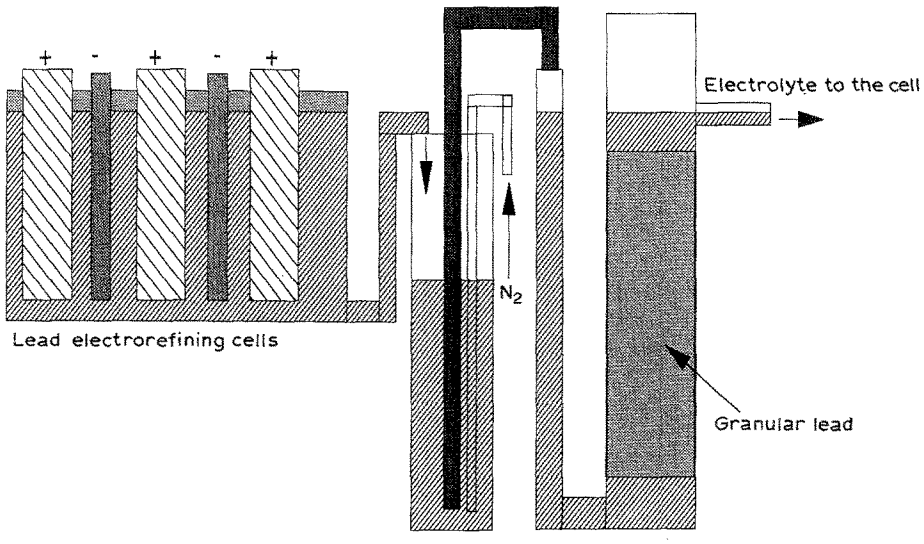

Fig. 11. Continuous purification of electrolyte via purification columm [125, 126].

ing wrinkles on the cathodes right after they are produced [79]. Procedures to avoid dross incorporation in the lead cathodes have also been developed [136]. In this section of the electrorefining process high levels of automation have been achieved [137].

5.3. *Cell electrolysis parameter optimization*

The overall electrorefining process has been studied using statistical correlations of some of the variables measurable in an operating plant [39, 54, 98]. To optimize the electrolysis parameters when the BEP is run at high current densities ($\geqslant 200\,A\,m^{-2}$), factorial design of experiments at three levels for four variables has been used by Lange *et al.* [98]. They varied $PbSiF_6$ and H_2SiF_6 concentrations, temperature, and current density, at constant values of addition agent (glue), anode composition, cell geometry, and electrolyte recirculation. The influence of these parameters on the average anodic and cathodic polarization, on the cell voltage, and on the specific energy consumption was obtained by employing regression analysis correlations. In addition, changes in these parameters were correlated with the cathode quality and appearance as well as with the consumption of glue. The optimum electrolysis parameters found for a current density increase (from 200 to $300\,A\,m^{-2}$) were a Pb^{+2} concentration of $60\,g\,l^{-1}$ (down from $80\,g\,l^{-1}$), a glue addition maximum of $1500\,g\,ton^{-1}$ of lead (up from $1250\,g\,l^{-1}$), a free H_2SiF_6 content of $120\,g\,l^{-1}$ (no change) and an electrolyte temperature of 35 to 40° C. Under these electrolysis conditions, Lange *et al.* found that antimony and bismuth slimes layers could be subjected to anodic polarizations as high as 280 mV without serious impairment of the cathode quality.

Optimization of the BEP through half cycle anode slimes scrubbing and cathodes exchange was also investigated by Lange *et al.* [98]. Not only did the specific energy consumption decrease by the implementation of this procedure, but highly pure cathodes were assured by avoiding anodic overpotentials in excess of the preset limits for impurities dissolution. On the other hand, the exchange of cathodes and the half cycle scrubbing of the anodes incorporates labour increases making implementation difficult. The use of this technique is necessary when anodes containing high impurity levels (> 5%) are to be treated. For example, in Russia [57], lead anodes containing as much as 15% bismuth are scrubbed every 48 h during the 6 day long anode cycle. In addition to this, cathodes are exchanged daily to avoid short circuits and to obtain a deposit of acceptable purity [57].

Lange *et al.* also studied the use of PCR in the BEP. Figure 12 shows the anodic overpotential dependance on the PCR parameters. Thiet [39] found that the use of PCR decreased the anodic overpotential values. The reduction in the anodic overpotential values did not reflect in lower PCR energy consumption probably because it was offset by unproductive energy consumption during the reverse current phase of the cycle. Thiet also showed that the quality of the PCR cathode deposits was very high [39].

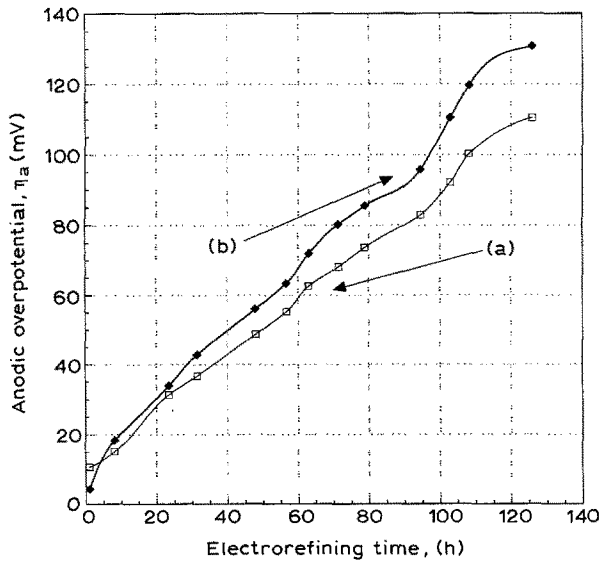

Fig. 12. Influence of the cycle length and current reversal ratio on the anodic overpotential value during PCR [39]: (a) $T_{forward}/T_{backward} = 11.5$, $T_{cycle} = 10$ s; (b) $T_{forward}/T_{backward} = 19$, $T_{cycle} = 20$ s.

5.4. *Bipolar refining of lead*

Among other alternatives to optimize the lead electrorefining process, the use of a bipolar configuration looks most promising. In this configuration only the terminal electrodes are connected to the source of current. Between these electrodes a large number of bipolar electrodes can be incorporated. One side of these electrodes will corrode anodically, while pure lead will deposit on the other side. The impurities will be left behind as a slimes layer on the anodic side. The advantages of operating the BEP in a bipolar mode include PCR, c.p.v., optimum lead and free acid contents, and the use of jumbo electrodes ($\sim 4\,m^2$, possible because there are no bus-bar connections)*. The process has been operated in a pilot plant where it proved to be superior to the parallel process [141]. The rationale for the current use of the parallel system is that a high economic investment is required for the substitution and implementation of the bipolar process. If new plants to electrorefine lead are to be constructed in the future, very likely they will be assembled on the bipolar configuration.

6. Conclusions

1. The Betts process for lead electrorefining is successful because it retains most noble impurities in adherent anode slimes while depositing rather pure (> 99.99%) lead cathodes. The anode slimes account for only 1 to 4% of the weight of dissolved lead, and so represent an enrichment of a factor of 25 to 100 in the noble

* In the Bipolar mode by-pass currents are reduced by increasing the area of the electrodes so that the ratio of bypass to electrode area in the cell decreases.

impurities (particularly precious metals) present in lead bullion.

2. The anode slimes are adherent and usually thick (> 1 cm). X-ray diffraction on these slimes identify mainly oxides and lead fluoride, but these results may have been compromised by accidental oxidation of samples. The actual (*in situ*) slimes are more likely electrically conducting filaments of noble metals and intermetallic compounds, sometimes supplemented by precipitated PbF_2 and SiO_2 (both of which have been detected in anode slimes precipitates).

3. It is well known that anode polarization must be limited to less than 200 mV to avoid Bismuth dissolution and transfer to the cathodic deposit. This together with the reported X-ray diffraction data provides evidence that *in situ* slimes contain metallic bismuth.

4. Electrolyte extracted from within slimes layers show that it is markedly enriched in lead fluosilicate and somewhat depleted in fluosilicic acid. The change in the inner slimes electrolyte concentration is more abrupt towards the slimes-anode interface and accounts for the hydrolysis of SiF_6^{-2} ions:

$$3Pb^{+2} + SiF_6^{-2} + 3H_2O \longrightarrow 3PbF_2 + H_2SiO_3 + 4H^+$$

5. Variations of the Betts lead refining process that have been incorporated include periodic current reversal (PCR) and bipolar refining.

6. Fundamental electrochemical studies have evaluated the effects of additives such as lignin sulphonates, glue, and aloes extracts as levelling agents in cathode deposition. The presence of these additives in the electrolyte for lead refining may affect both the cathodic and the anodic overvoltages.

Acknowledgement

This work was supported financially through a National Autonomous University of Mexico (U.N.A.M.) Graduate fellowship and through supplementary funding from the Natural Sciences and Engineering Research Council of Canada (Grant # A2450).

References

[1] A. T. Hodge, *Sci. Am.* **252** (6) (1985) 114.
[2] N. H. Gale and Z. Stos-Gale, *ibid.* **244** (6) (1981) 176.
[3] D. H. Ward, The AusIMM G. K. Williams Memorial Symposium, Scientific and technological developments in extractive metallurgy [Proc. Conf.], Symposia Series No. 43, Australia (1985) p. 25.
[4] S. J. Pedley, R. Widmark, A. O. Adami, H. Maczek, G. Althabegoity, J. D. Bendit and S. A. Hiscock, *Tr. Inst. Min. Met. A* **92** (1983) 135A.
[5] C. A. Sutherland, *CIM Bull.* **81** (1988) 85.
[6] T. R. A. Davey, 'Lead-Tin-Zinc '80' [Proc. Conf.] (edited by J. M. Cigan, T. S. Mackey and T. J. O'Keefe), AIME Symposium (1980) p. 477.
[7] Anonymous, United Nations, 'Industrial Development Organization Vienna: Technological Developments in Lead and Zinc Products and their significance to Development Countries' (1969) chapter 7.
[8] R. Kleinert, *Erzmetall.* **22** (1969) 327. (Translation National Translations Center, NTC 11F-81-22057.)
[9] T. Nakamura, F. Noguchi, Y. Ueda and H. Ito, The AusIMM Adelaide Branch, Research and Development in Extractive Metallurgy [Proc. Conf.], Australia (1987) p. 85.
[10] G. C. Quigley and J. V. Happ, *ibid.*, p. 187.
[11] J. N. Greenwood, *Metall. Rev.* **6** (1961) 279.
[12] L. Gmelins 'Handbuch der Anorganischen Chemie', Verlag Chemie – GMBH, Weinheim-Bergstrasse, Germany, System No. 47 Pb [B2] (1972) 364–369.
[13] I. Molnar, Z. Horvarth and I. Meszaros, *Magy. Alum.* **21** (1984) 413 and **22** (1985) 189.
[14] M. Wada and T. Kobayashi, *Nippon Kogyo Kaishi* **90** (1035) (1974) 370.
[15] S. Tasai and T. Tanaka, *Bull. Fac. Eng. Hokkaido Univ.* **122** (1984) 1.
[16] M. Fujimori, H. Imazawa, T. Osawa and K. Baba, Mineral Processing and Extractive Metallurgy [Proc. Conf.] (edited by M. P. Jones and P. Gill), The Institution of Mining and Metallurgy, London (1984) p. 421.
[17] L. Chuanyan and Z. Peihua, *ibid.* p. 699.
[18] T. Tanaka, *Bull. Fac. Eng. Hokkaido Univ.* **48** (1968) 25.
[19] Y. Hoh, B. Lee, T. Ma, W. Chuang and W. Wang, European Patent Application, Applic. No. 81 301 045.1, filed 12 March 1981, Int. Cl. C22 B 3/00, C22 B B/04.
[20] R. Guerreiro, E. Sentimenti and I. Vittadini, UK Patent Application GB 2 118 536A, filed 23 March 1983.
[21] T. Tanaka and T. Midorikawa, *J. Less-Common Met.* **15** (1968) 201.
[22] S. Dianbang, Mineral Processing and Extractive Metallurgy [Proc. Conf.] (edited by M. P. Jones and P. Gill), The Institution of Mining and Metallurgy, London (1984) p. 599.
[23] D. S. Flett, *Trans. Instn. Min. Metall. C* **94C** (1985) 232.
[24] M. M. Wong, F. P. Haver and R. G. Sandberg, 'Lead-Tin-Zinc '80' (edited by J. M. Cigan, T. S. Mackey and T. J. O'Keefe), AIME Symposium (1980) p. 445.
[25] J. M. Demarthe and A. Gorgeaux, *ibid.* p. 426.
[26] A. Y. Lee, A. Wethington and E. Cole Jr., US Bureau of Mines, RI 9055 (1986).
[27] A. G. Betts, 'Lead Refining by Electrolysis', Wiley & Sons, New York (1908).
[28] *Idem*, US Patent 713 277, 9 January 1902.
[29] *Idem*, US Patent 713 278, 9 October 1902.
[30] *Idem*, US Patent 918 647, 23 January 1907.
[31] *Idem*, US Patent 891 395, 8 December 1906.
[32] *Idem*, US Patent 126 576, 9 October 1902.
[33] D. L. Thomas, C. J. Krauss and R. C. Kerby, TMS paper selection A81-8, TMS-AIME, Warrendale, PA (1981).
[34] P. F. McIntyre, *Trans. Amer. Inst. Min. Metall. Engrs.* **121** (1936) 271–82.
[35] Anonymous, *Cominco Magazine* **23** (1962) 17–21.
[36] J. B. Hutl, *Eng. Min. J.* **139** (1938) 34.
[37] L. Zhenya, Non-Ferrous Metals (China) **37** (1985) 53.
[38] W. Mao-Chuan, *Metall (Berlin)* **35** (1981) 425.
[39] N. K. Thiet, Ph.D. Dissertation, Bergakademie Freiberg, East Germany (1982).
[40] E. R. Freni, *J. Met.* **17** (1965) 1206.
[41] G. Tremolada and L. Abduini, Symposium on Sulphamic Acid and its Electrometallurgical Applications, Milan (1967) p. 353.
[42] E. P. Freni, *Erzmetall.* **22** (1969) 312; also in supplementary volume (1969) p. 128.
[43] E. Nomura, A. Aramaki and Y. Nishimura, TMS paper selection A74-21, TMS-AIME, Warrendale, PA (1974).
[44] S. Hirakawa, E. Nomura, T. Mori and Y. Hirayama, TMS paper selection A78-14, TMS-AIME, Warrendale, PA (1978).
[45] E. Nomura, Y. Nakamura, K. Takahashi, N. Ueda, TMS paper selection A81-7, TMS-AIME, Warrendale, PA (1981).
[46] A. Ohta, A. Ichinose and T. Kohno, TMS paper selection A81-21, TMS-AIME, Warrendale, PA (1981).
[47] K. Tadao and K. Yoshiaki, TMS paper selection A81-9, TMS-AIME, Warrendale, PA (1981).
[48] M. Wada, K. Hashimoto, K. Ono-ike, *Nippon Kogyo Kaishi* **97** (1981) 400.
[49] Y. Sugawara and S. Ishii, *Metall. Rev. MMIJ* **2** (1985) 90.
[50] N. Hamabe, S. Kawakita and E. Oshima, *ibid.* **2** (1985) 102.
[51] J. Minoura and Y. Maeda, *ibid.* **1** (1984) 138.
[52] T. E. Harper, *Trans. Amer. Inst. Min. Metall. Engrs.* **121** (1936) 283–88.

[53] T. E. Harper and G. Reinberg, *Eng. Min. J.* **136** (1935) 119.
[54] C. A. Aranda and P. J. Taylor, AIME World Symposium of Mining and Metallurgy of Lead and Zinc (edited by C. H. Cotterill and J. M. Cigan) (1970) p. 891.
[55] J. S. Jacobi, Refining Process in Metallurgy [Proc. Conf.], Verlag Chemie, Weinheim (1983) p. 12–20.
[56] Anonymous, *Chem. Proc.* (*London*) **15** (1969) 18.
[57] E. Lach and M. Kwarcinski, *Rudy i Met. Niezelaz* **29** (1984) 258.
[58] M. Barak, *Chem. and Ind.* (*London*) (1976) 871.
[59] J. Encev, *Metalurgija* (*Sofia*) **4** (1973) 25.
[60] C. L. Mantell, 'Industrial Electrochemistry', McGraw-Hill, New York (1950) p. 314–22.
[61] K. Emicke, G. Holzapfel and E. Kuiprath, AIME World Symposium of Mining and Metallurgy of Lead and Zinc (edited by C. H. Cotterill and J. M. Cigan) (1970) p. 867.
[62] K. Emicke, G. Holzapfel and E. Kuiprath, *Erzmetall.* **24** (1971) 205. (Translation National Translations Center, NTC 11F-81-11544).
[63] Private Communication, Drs Kartenbeck and Traulsen, Norddeutsche Affinerie (19 January 1988).
[64] A. S. Kafka, *Eng. Min. J.* **190** (1989) 27.
[65] C. J. Chen and C. C. Wan, *J. of Fluorine Chem.* **27** (1985) 167.
[66] F. Beck, *Werkst. Korros.* **28** (1977) 688.
[67] H. Silman, Galvanotechnisches Kolloqium., 6th (1980) p. 79.
[68] U. Dacati, P. Cavalloti and D. Colombo, Electrochemical Process and Plant Design [Proc. Conf.] (edited by R. C. Alkire, T. R. Beck and R. D. Varjian) The Electrochemical Society (1983) p. 110.
[69] U. Ginatta, TMS paper selection A85-29, TMS-AIME Warrendale, PA (1985).
[70] M. Maja, N. Penazzi, P. Spinelli, M. V. Ginatta, U. Ginatta and G. Orsello, IChem Symposium Series NO. 98 (1986) p. 173.
[71] M. Ginatta, UK Patent Application GB 2 121 826A, filed 13 May 1983, published 4 January 1984.
[72] M. Ginatta, UK Patent Application GB 2 121 437A, 21 December 1983.
[73] E. R. Freni, in Symposium on Sulphamic Acid and its Electrometallurgical Applications, Milan (1967) p. 367.
[74] P. M. Strocchi, R. Peruzzi, A. Rozzoli, D. Sinigaglia and B. Vicentini, *Electrochim. Met.* **2** (1967) 95.
[75] A. La Vecchia, P. Pedeferri, R. Peruzzi, A. Porta and D. Sinigaglia, *ibid.* **1** (1966) 255.
[76] P. Pedeferri and A. La Vecchia, *ibid.* **1** (1966) 112.
[77] P. M. Strocchi, R. Peruzzi, A. Rozzoli, D. Sinigaglia and B. Vicentini, *ibid.* **2** (1967) 95.
[78] T. Konada, Y. Tenmaya and K. Yamaguchi, CIM Symp. on Quality Control in Non-Ferrous Pyrometallurgical Processes [Proc. Conf.], Vancouver B.C. (1985) pp. 2–13.
[79] E. Nomura, M. Aramaki and Y. Nishimura, US Patent 3 960 681, 1 June 1976.
[80] L. Gmelins 'Handbuch der Anorganischen Chemie', Verlag Chemie–GMBH, Weinheim-Bergstrasse, Germany, System No. 15 Si [B] (1959) 614–653.
[81] C. J. Krauss, *J. Met.* **28** (1976) 4.
[82] Private Communication, H. Shouyi, Shenyang Smelter, 21 January 1988.
[83] Private Communication, C. J. Krauss, Cominco Ltd., 15 February 1988.
[84] Private Communication, Dr. Wegerdt, 'Albert Funk' Metallurgical Complex, 2 March 1988.
[85] Private Communication, N. Córdova, S., Empresa Minera del Centro de Perú, 28 January 1988.
[86] Private Communication, H. Kubo, Kamioka Mining Co. Ltd., 10 January 1988.
[87] C. J. Krauss, Canadian Patent 1 020 491, 8 November 1977.
[88] I. D. Entchev, N. T. Kuntchev, G. A. Haralampiev, A. D. Milkov, B. Y. Sotirov and D. A. Petrov, Canadian Patent 928 246, 12 June 1973.
[89] Bulletin of Alloy Phase Diagrams, **1** (1980) 56.
[90] *Ibid.* **1** (1980) 62.
[91] *Ibid.* **2** (1981) 81.
[92] *Ibid.* **2** (1981) 86.
[93] M. Hansen, 'Constitution of Binary Alloys', 2nd ed., McGraw-Hill, New York (1958) pp. 41, 173, 325 and 1101.
[94] T. Tanaka, *Metall. Trans. B* **8B** (1977) 651.
[95] R. Elliot, 'Eutectic Solidification Processing, Butterworths, London (1983).
[96] Y. Nishimura, Canadian Patent 1 019 132, 18 October 1977.
[97] F. Wenzel and K. Hein, *Neue Hütte* **19** (1974) 263. (Translation National Translations Center, NTC 11F-81-11594.)
[98] H. J. Lange, K. Hein and N. K. Thiet, *ibid.* **28** (1983) 136.
[99] H. J. Lange, K. Hein and D. Schab, *Freiberg. Forschungsh. B.* **B195** (1977) 29. (Translation NRC 2873873.)
[100] K. Hein, *Chem. Technol.* (*Leipzig*) **36** (1984) 378.
[101] H. Bombach, K. Hein, J. Korb and H. J. Lange, *Neue Hütte* **31** (1986) 347. (Translation MINTEK TR-1265.)
[102] B. G. Ateya and H. W. Pickering, *J. Appl. Electrochem.* **11** (1981) 453.
[103] J. M. Hornut, G. Valentin and A. Storck, *J. Appl. Electrochem.* **15** (1985) 237.
[104] O. Wein, *Collect. Czech. Chem. Commun.* **53** (1988) 697.
[105] M. Jaskula, *Erzmetall.* **42** (1989) 117.
[106] M. Maeda, *J. Electrochem. Soc. Jpn* (Overseas Suppl. Ed.) **26** (1958) E 21.
[107] L. Kiss, 'Kinetics of Electrochemical Metal Dissolution', Studies in Physical and Theoretical Chemistry 47, Elsevier, Hungary (1988).
[108] G. A. Kuznetsova, *Tsvetn. Metall.* **8** (1967) 69.
[109] L. I. Reznichenko and A. D. Pogorelyi, *Sov. Non-Ferrous Met. Res.* (Engl. Transl.) **4** (1976) 226.
[110] L. I. Reznichenko, *ibid.* **5** (1977) 245.
[111] W. Eisert, *Neue Hütte* **4** (1959) 29.
[112] I. Pajak, M. Kwarcinski, A. Bojanowska and B. Kwarcinska, *Pr. Inst. Met. Nieze* **5** (1976) 121.
[113] P. Mechenov, *Minno Delo Met.* [*Sofia*] **17** (1962) 30. Chemical Abstracts: 57 (1962) 14776.
[114] F. Wenzel, *Neue Hütte* **18** (1973) 374.
[115] F. Wenzel, Ph.D. Dissertation, Bergakademie Freiberg, East Germany (1971).
[116] M. Isawa and T. Tanaka, *Nippon Kogyo Kaishi* **77** (1961) 483.
[117] *Idem, ibid.* **78** (1962) 519.
[118] F. Miyashita and G. Miyatani, *Technol. Rep. Kansai Univ.* **13** (1972) 81.
[119] *Idem, ibid.* **14** (1973) 61.
[120] *Idem, ibid.* **18** (1977) 87.
[121] *Idem, Nippon Kogyo Kaishi* **90** (1974) 617.
[122] *Idem, ibid.* **92** (1976) 431.
[123] *Idem, ibid.* **94** (1978) 485.
[124] S. Hirakawa and R. Oniwa, Canadian Patent 1 023 691, 3 January 1978.
[125] G. Baralis, Lead 65 [Proc. Conf.], Arnhem (1967) p. 317.
[126] G. Baralis and M. Marone, *Metall. Ital.* **7** (1967) 494.
[127] R. C. Kerby and H. E. Jackson, *Can. Metal. Quart.* **17** (1978) 125.
[128] R. C. Kerby, Canadian Patent 1 115 658, 5 January 1982.
[129] C. J. Krauss and G. Shaw, Canadian Patent 988 897, 11 May 1976.
[130] T. N. Andersen, R. C. Kerby and T. J. O'Keefe, *J. Met.* **37** (1985) 36.
[131] R. C. Kerby and C. J. Krauss, Lead-Tin-Zinc '80 [Proc. Conf.] (edited by J. M. Cigan, T. S. Mackey and T. J. O'Keefe), AIME Symposium (1980) p. 187.
[132] J. Ambrose and B. Conard, CANMET Contract serial No. ISQ 85-00148, 15 September 1986.
[133] 'Applications of Polarization Measurements in The Control of Metal Deposition' (edited by I. H. Warren), Elsevier, Amsterdam (1984).
[134] C. T. Wang, Ph.D. Dissertation, The University of Missouri, Rolla (1983).
[135] D. M. Hembree Jr., *Plat. Surf. Finish* **73** (1986) 54.
[136] S. Tokunobu, Canadian Patent 1 001 379, 18 February 1974.
[137] H. J. Lange and D. Kappler, *Freiberg. Forschungsh. B.* **B210** (1979) 171.
[138] R. C. Kerby and C. J. Krauss, US Patent 4 416 746, 22 November 1983.
[139] R. C. Kerby, Canadian Patent 1 174 198, 11 September 1984.
[140] *Idem*, Canadian Patent 1 126 684, 29 June 1982.
[141] R. C. Kerby and R. D. H. Willans, TMS paper selection A84-15, TMS-AIME, Warrendale, PA (1984).
[142] M. Kwarcinski, A. Bednarek, T. Nalawajek and A. Kurzeja, *Rudy i Met. Niezelaz.* **29** (1984) 295.